DEVELOPMENTAL DYNAMICS 211:11–25 (1998)

Insulin-Like Growth Factor II Receptor, Transforming Growth Factor-β, and Cdk4 Expression and the Developmental Epigenetics of Mouse Palate Morphogenesis and Dysmorphogenesis

MICHAEL MELNICK,[1]* HAIMING CHEN,[1] SUSAN BUCKLEY,[2] DAVID WARBURTON,[2] AND TINA JASKOLL[1]
[1]*Laboratory for Developmental Genetics, University of Southern California, Los Angeles, California*
[2]*Department of Surgery, Children's Hospital of Los Angeles, Los Angeles, California*

ABSTRACT **The B10/B10.A congenic mouse pair serves as a model for identifying specific genes related to morphogenesis and dysmorphogenesis of the embryonic palate and other organs. The present report describes our initial investigation of the Fraser-Juriloff paradigm, which proposes that susceptibility to malformation results from genetically determined differences in normal developmental patterns. Specifically, we evaluated the relationship between *Igf*2r gene expression, transforming growth factor-β (TGF-β) activation, and *cdk*4 gene expression. By using in situ hybridization, RNase protection assays, indirect immunofluorescence, Western blots, and bioassays, we show 1) the presence of insulin-like growth factor II (IGF-II), IGF-II receptor (IGF-IIR), IGF-IR, TGF-β, plasminogen, plasminogen activators [urokinase plasminogen activator (uPA) and tissue plasminogen activator (tPA)], and Cdk4 in developing palates; 2) on embryonic day 14 (E14), which is a critical day for palatal growth, B10.A embryos have 82% greater IGF-IIR mRNA than B10; 3) on E14, B10.A embryonic palates have a 57% greater level of *active* TGF-β2 than B10, although the total TGF-β2 is nearly identical; and 4) on E14, B10 embryonic palates have a 52% greater level of Cdk4 mRNA than B10.A palates, a measure of cell cycle progression. Because cellular activation of *latent* TGF-β appears to require binding to the mannose-6-phosphate (M6P) binding site of the IGF-IIR and is plasmin and plasminogen activator dependent, the positive correlation of IGF-IIR levels and active TGF-β2 levels seems to be key. Thus, the strain variation of TGF-β2/IGF-IIR-mediated growth inhibition in late G_1 phase would appear to account for the slower growth and development of B10.A palates relative to B10. Elevated corticosteroid (CORT) exposure in E14 B10.A embryos significantly increases TGF-β levels, 87% of which is TGF-β2, as well as the levels of active TGF-β, 64% of which is TGF-β2. Without exogenous CORT, B10.A embryos do not have clefts; hence, we present an *outline of pathogenesis*: slower growing B10.A embryos have an up-regulation of IGF-IIR, which serves to sequester IGF-II from the growth-promoting IGF-IR and to bind more CORT-up-regulated, latent TGF-β2 for subsequent plasmin-dependent activation; higher levels of TGF-β2 signaling down-regulate Cdk4 and result in greater palatal growth inhibition at a critical stage of palatogenesis and, thus, cleft palate. We present an epigenetic model of information processing related to cell proliferation. The model is a dynamical network that uses continuous logic to learn its rules from changing conditions. *Dev. Dyn. 1998;211:11–25.***

Key words: insulin-like growth factor type II receptor; transforming growth factor-β; Cdk4; mouse genetics; palate morphogenesis; cleft palate

INTRODUCTION

The etiology and pathogenesis of human nonsyndromic cleft palate (CP) is still largely an enigma. Unquestionably, both genetic and environmental factors play a role in initiating this common malformation. The present report describes our initial investigation in mice of the Fraser-Juriloff paradigm, which proposes that susceptibility to malformation results from genetically determined differences in normal developmental patterns (Fraser, 1980). Specifically, we investigated the relationship between *Igf*2r gene expression, transforming growth factor-β (TGF-β) activation, and *cdk*4 gene expression vís-a-vís known normal developmental variation and glucocorticoid-induced CP in H-2 congenic mouse strains.

Palatogenesis

The mammalian palate begins development from projections of the paired maxillary processes of the first branchial arches, termed palatal shelves (or lateral

Grant sponsor: National Institutes of Health; Grant numbers: DE 12111, DE 07006, DE 10376, HL 44060, and HL 44977.
*Correspondence to: Dr. Michael Melnick, Laboratory for Developmental Genetics, University of Southern California, 925 West 34th Street, DEN 4266, MC-0641, Los Angeles, CA 90089-0641.
Received 23 June 1997; Accepted 24 September 1997

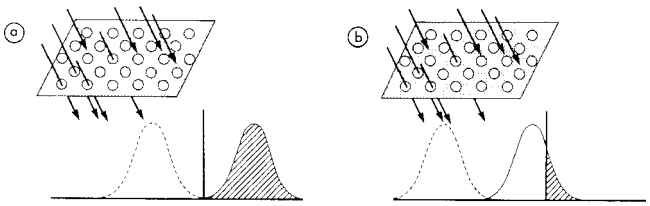

Fig. 1. **a,b:** Fraser-Juriloff model of cleft palate (CP) susceptibility (Fraser, 1980). For details, see text. Reprinted with permission of John Wiley & Sons, Inc.

palatine processes). Initially, these shelves are in a vertical position on each side of the developing tongue, but, as the mandible grows, the tongue moves downward, and the shelves become horizontal and grow toward each other. Subsequently, the shelves grow sufficiently large to approximate one another and begin to fuse. During fusion, the apposed epithelia form an epithelial seam, which undergoes apoptosis, migration, and/or transformation and results in mesenchymal continuity (for a general review, see Melnick et al., 1982).

Thus, palate formation is complex, and there are numerous potential untoward possibilities, the most common being delayed shelf horizontalization and inadequate shelf growth (Melnick and Shields, 1982). It has long been clear that human CP is associated with major genes, although it is not classically Mendelian (Shields et al., 1981). Mouse models dating back to the 1950s (Fraser and Fainstat, 1951) indicate that CP manifestation depends on major gene effects and exposure to aberrant environments in utero. A recent study by Christiansen and Mitchell (1996) supports the mouse models, concluding that, in human CP, there are probably two or three loci related to susceptibility; that these loci effect synergistic action and/or interact with important environmental factors; and that, given this complexity, "traditional linkage studies of CP will be heroic undertakings." Thus, we have always to return to the *inbred* mouse for clues, not least because the huge genetic variation in *outbred* populations (humans) make it exceedingly difficult to detect complex disease genes.

Mouse Models of CP

Figure 1 presents the Fraser-Juriloff paradigm (Fraser, 1980) of strain differences in susceptibility to an environmental teratogen resulting from a genetically determined difference in normal developmental pattern. The roof with holes in it represents the maternal barrier between teratogen (Fig. 1, arrows) and embryo. The x-axis represents the phenotypic distribution, normal to the left of the vertical threshold and abnormal to the right; the threshold separates palate closure from palate nonclosure. In Figure 1a, palate closure is normally late (*slow growth*), so the phenotypic distribution for this genotype (Fig. 1a, dashed curve) is near the threshold, and the delaying effect of the teratogen causes all embryos (Fig. 1a, solid curve) of this genotype to fall beyond the threshold and be affected (Fig. 1a, hatched area). In an early closing (*faster growth*) genotype (Fig. 1b), the same delay causes a minority of embryos to be affected. Of course, these two cases are the outer boundaries of the model, and there will be many genotypes (Fig. 1, dashed curves) at varying distances to the left of the threshold.

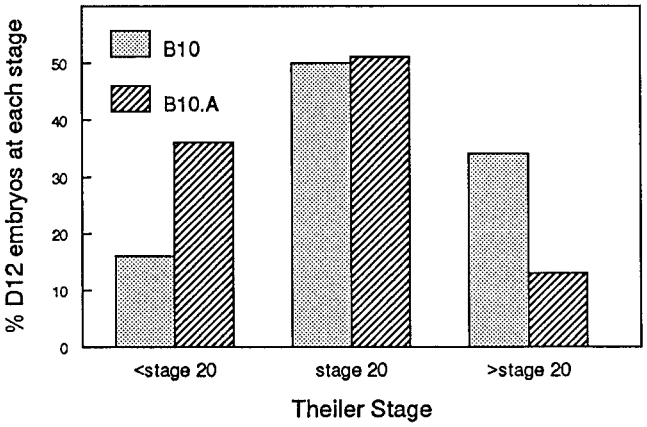

Fig. 2. Theiler staging of B10 and B10.A embryos on day 12 of gestation, when 50% of both B10 and B10.A embryos are at stage 20. However, there is a significantly greater percentage of B10.A embryos at less than stage 20 compared with B10 embryos, and a significantly smaller percentage of B10.A embryos are at greater than stage 20 compared with B10 embryos.

The exposure of embryonic mice to corticosteroids (CORT) has long been known to result in CP (Fraser and Fainstat, 1951). Studies in our laboratory and other investigators have shown consistently that CORT-induced CP is related to genetic variation at or near the H-2 complex on mouse chromosome 17 (Bonner and Slavkin, 1975; Gasser et al., 1991; Goldman, 1984; Melnick et al., 1981a). H-2 congenic mouse strains share identical genetic backgrounds, with the exception of a 3–18 cM region of chromosome 17 (i.e., the congenic region), which encompasses the H-2 complex and defines each H-2 haplotype (Vincek et al., 1990); they represent an important tool for investigating the contribution of specific congenic genes to development. By using H-2 congenic mice, we have shown that B10.A ($H\text{-}2^a$) mice are ninefold more susceptible to CORT-induced CP than B10 ($H\text{-}2^b$) mice; reciprocal hybrid studies have demonstrated a significant but much weaker maternal effect (Melnick et al., 1981a). More recently, we have shown that CORT-induced delay in the normal down-regulation of TGF-β2 transcription is a key event in the pathogenesis of CORT-induced CP in B10.A embryos (Jaskoll et al., 1996a). In the present investigation, we sought a link between genes on chromosome 17 and TGF-β2, the gene for which is on chromosome 1.

H-2 haplotype-specific differences in the rate of embryonic development in B10.A and B10 congenic mice have been studied extensively in our laboratory. Significant strain differences ($P < 0.025$) in the number of embryonic day 12 (E12) embryos that reach the appropriate Theiler stage (Theiler, 1989) are seen routinely (Fig. 2).

In addition, B10.A mice produce smaller embryos, with delayed palatal development, lung maturation, H-2 antigen expression, and skeletal development compared with B10 mice at identical Theiler stages (Good et al., 1991; Hu et al., 1990; Jaskoll et al., 1991; Melnick and Jaskoll, 1992; Melnick et al., 1981b, 1982). Thus, if CORT inhibits palatogenesis to the same degree in both strains via TGF-β2 regulation (Jaskoll et al., 1996a), then it is not surprising that the slower developing B10.A embryo is more vulnerable to abnormal palatogenesis than the faster developing B10 embryo, as predicted by the Fraser-Juriloff paradigm (Fig. 1).

Our present study indicates that one genotypic element of this etiologic equation is the gene for insulin-like growth factor II receptor (IGF-IIR); *Igf*2r is located at approximately map position 8.0 on chromosome 17, centromeric to the H-2 complex. IGF-IIR-mediated negative regulation of IGF-II ligand plays a critical role in IGF-II-dependent embryonic growth and development (Ellis et al., 1996; Lau et al., 1994; Melnick et al., 1996; Wang et al., 1994). Furthermore, TGF-β activation, in part, is dependent on *latent* TGF-β binding to IGF-IIR (Dennis and Rifkin, 1991; Gleizes et al., 1997). We report here a positive correlation between IGF-IIR and *activated* TGF-β2 levels and a negative correlation between those two molecules and Cdk4 levels, a measure of progression through the cell cycle to division. In sum, these findings add quantitative molecular details to the genetically determined threshold phenomenon of the Fraser-Juriloff paradigm and provide clues to the etiology of human CP.

RESULTS

IGF-IIR Analysis

A sequential series of qualitative and quantitative studies was initiated to characterize *Igf*2r expression in the B10/B10.A congenic mouse pair. B10.A and B10 embryos had comparable outcomes at comparable stages of palatal development, although the B10.A embryonic palatal shelves elevate and fuse slightly later than B10 on average. First, we determined the spatial distribution of IGF-II, IGF-IR, and IGF-IIR protein with progressive palatal development (E12.5 to E15.0) by using indirect immunofluorescence (Figs. 3–5). The presence of IGF-II, IGF-IR, and IGF-IIR in all cellular types of the embryonic palate suggests that the IGF-II signal-transduction pathway (IGF-II + IGF-IR → cell division) and the IGF-IIR negative regulation of the IGF-II pathway are involved in regulating palatal growth.

Second, we investigated the presence of IGF-IIR transcripts in developing palates by in situ hybridization (Fig. 6); transcripts are present in the palatal epithelium and throughout the mesenchyme. Third, we

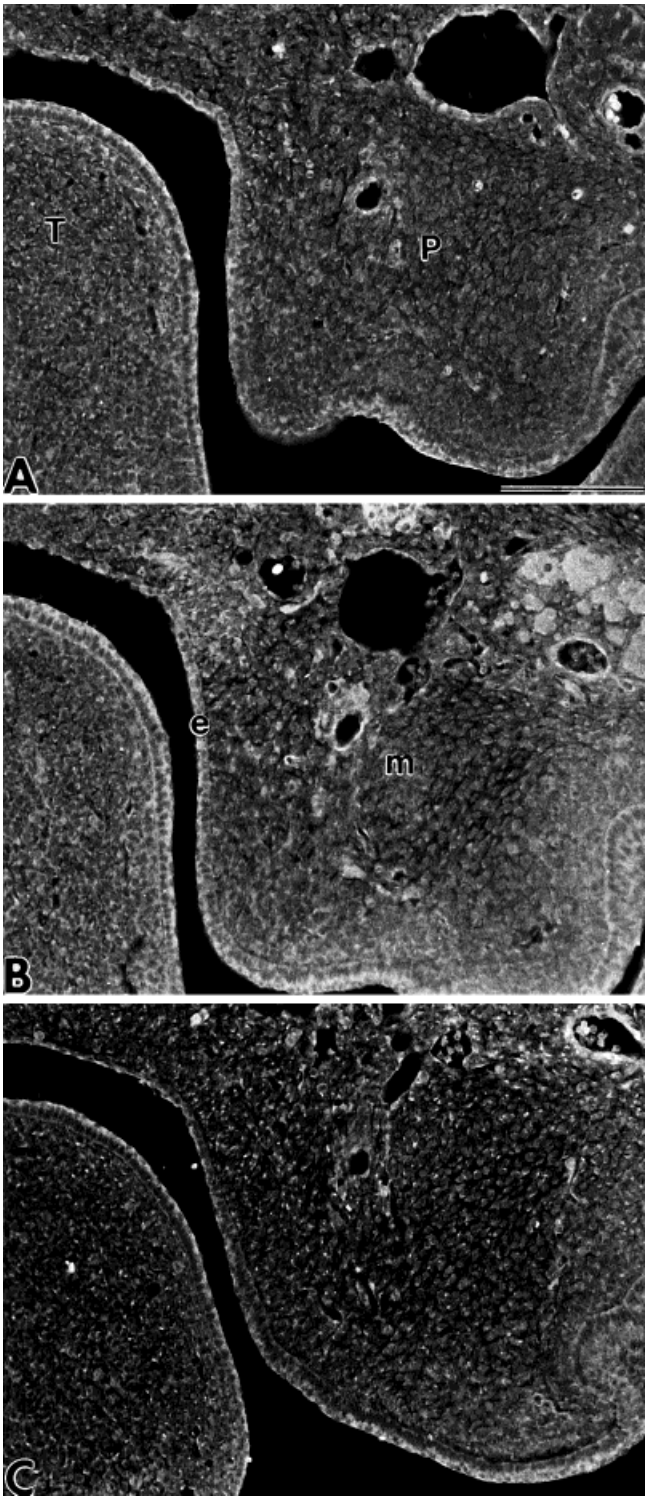

Fig. 3. Distribution of insulin-like growth factor II (IGF-II), insulin-like growth factor I receptor (IGF-IR), and IGF-IIR in early (embryonic day 12.5; E12.5) B10.A mouse palates. Palate development consists of vertical palatal shelves lateral to the tongue (T) that elevate and rotate to a horizontal position, followed by palatal shelf growth and fusion. In the early vertical palatal shelves (P), IGF-II, IGF-IR, and IGF-IIR are localized in the epithelia (e) and mesenchyme (m). **A:** IGF-II is immunolocalized primarily in the oral epithelium and is distributed sparsely throughout the mesenchyme. **B:** IGF-IR is immunolocalized in the epithelia and throughout the mesenchyme. **C:** IGF-IIR is distributed sparsely throughout the mesenchyme, and, to a lesser extent, it is also detected in the epithelium. Scale bar = 100 μm.

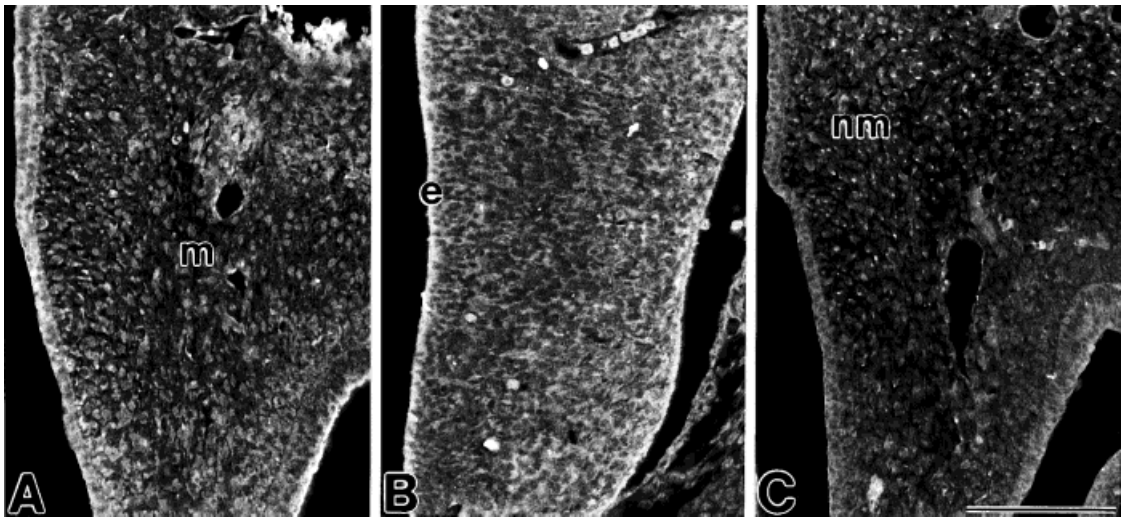

Fig. 4. Distribution of IGF-II (**A**), IGF-IR (**B**), and IGF-IIR (**C**) in later (E14) B10.A mouse vertical palatal shelves. In the later vertical shelves, the cell-specific distribution of IGF-II, IGF-IR, and IGF-IIR is similar to that seen in the early embryo. IGF-II and IGF-IR are immunodetected in the epithelium and in the mesenchyme. IGF-IIR is immunolocalized primarily in the mesenchyme adjoining the presumptive nasal epithelium and, to a lesser extent, in the epithelium. nm, mesenchyme adjacent to presumptive nasal epithelium; e, epithelium; m, mesenchyme. Scale bar = 100 μm.

quantitated IGF-IIR mRNA transcripts in B10 and B10.A E13–E15 palates (six litters/group) by RNase protection assay (Fig. 7). There is no significant change in transcript levels in B10 embryos with increasing gestational age. On E13 and E15, B10.A transcript levels are not significantly greater than those in B10 embryos; however, on E14, which is a critical day for palatal growth in these strains, B10.A embryos have an 82% greater level of IGF-IIR transcript than B10 embryos ($t_{10} = 2.41$; $P < 0.05$). Our results correlate well with the known slower growth and development of B10.A embryos compared with B10 embryos and the role IGF-IIR is thought to play in this regard (see Discussion and Fig. 13).

Fourth, in a separate experiment with E14 embryos (five or six litters/cross), matroclinus reciprocal hybrid crosses were compared along with B10 and B10.A incrosses for IGF-IIR mRNA transcript levels. There was no evidence of a maternal effect: The B10.A incross had approximately 60% greater IGF-IIR levels than the other three possible crosses ($t_{10} = 3.53$; $P < 0.01$), which were equivalent to one another.

TGF-β2 Analysis

Because 1) TGF-β2 appears to play a key role in palatal growth and development (Jaskoll et al., 1996a), 2) IGF-IIR binding is important for activation of latent TGF-βs (Dennis and Rifkin, 1991), and 3) E14 is a critical day for palatal growth as well as for the expression of TGF-β2 and IGF-IIR vís-a-vís strain differences (Jaskoll et al., 1996a; present study), we undertook a quantitative protein analysis of latent and activated TGF-β2 in B10 and B10.A E14 embryos (Figs. 8, 9). There are no substantial differences between congenic strains for total TGF-β, the mean palatal levels being nearly equivalent (Fig. 8). Approximately 20% of the total TGF-β is activated TGF-β (see data in Figs. 8, 9), and approximately 61% of the total activated TGF-β is activated TGF-β2 (Fig. 9). What is particularly striking is the 37% greater level of active total TGF-β in B10.A palates relative to B10 palates and the 57% greater level of active TGF-β2 (Fig. 9).

Because it has been shown that TGF-β2 mRNA is elevated on E14 in palates exposed to increased CORT levels (Jaskoll et al., 1996a), we repeated the above study with B10.A E14 embryos first exposed to increased CORT levels on E12 (Figs. 8, 9). Regarding total TGF-β, there was a 62% increase in total TGF-β levels in B10.A CORT-treated palates ($t_8 = 2.68$; $P < 0.05$), and 18% of this was activated; there was a 56% increase in total TGF-β2 levels ($t_8 = 2.71$; $P < 0.05$), and 64% of this was activated. Thus, elevated CORT exposure in utero significantly increases palatal TGF-β levels, 87% of which is TGF-β2, and the levels of activated TGF-β, 64% of which is TGF-β2.

IGF-IIR-dependent cellular activation of latent TGF-βs requires plasmin and plasminogen (Plg) activators, which activate plasminogen to plasmin (Dennis and Rifkin, 1991). Embryonic tissues are known to express Plg, urokinase plasminogen activator (uPA), and tissue plasminogen activator (tPA; Carroll et al., 1994; Häckel et al., 1995; Smokovits, 1980); Western blot analysis demonstrates that all three are present in developing E14 mouse palates (Fig. 10).

Cdk4 Analysis

Cyclin D-Cdk4 complexes mediate retinoblastoma protein (RB) phosphorylation, which frees the RB-complexed transcription factor, E2F, to activate genes required for G_1-S transition and DNA replication;

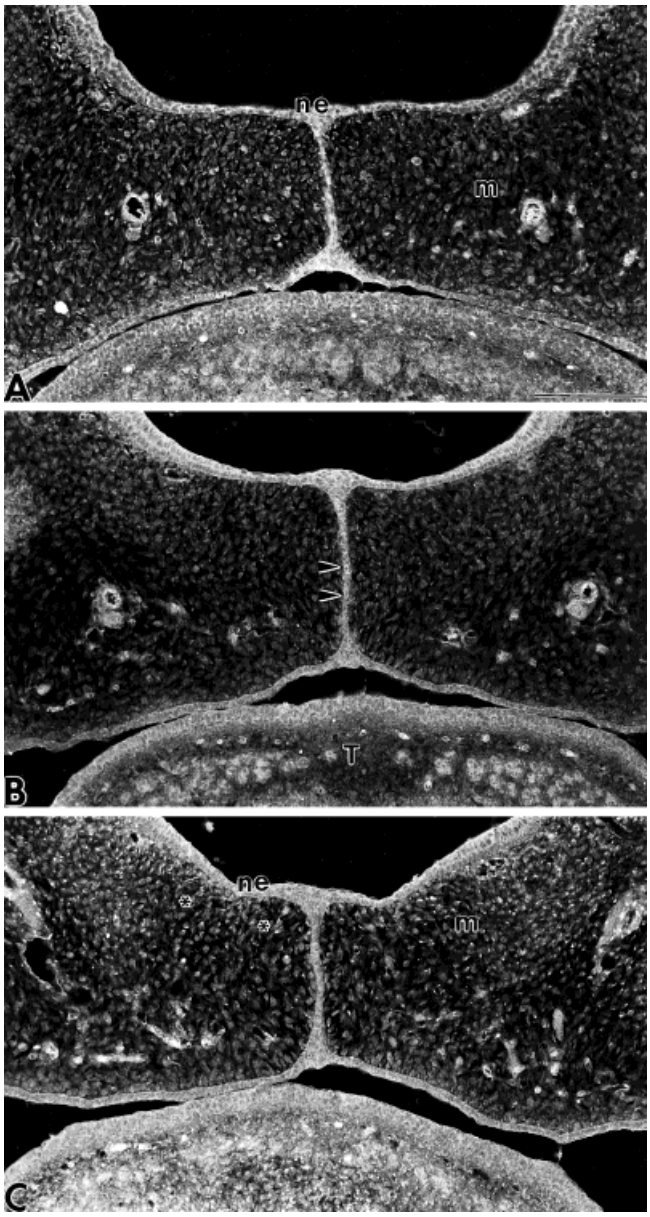

Fig. 5. Distribution of IGF II (**A**), IGF-IR (**B**), and IGF-IIR (**C**) in fusing E15 B10.A mouse palates. With development, the palatal shelves have elevated, have become horizontal, and have enlarged to fuse at the midline. In the fusing palatal shelves, IGF-II and IGF-IR are localized primarily to the epithelia (e). Compared with earlier stages (see, e.g., Fig. 4), there is an apparent decrease in IGF-II and IGF-IR immunolocalization in the mesenchyme (m). IGF-IIR is immunolocalized in the mesenchyme (asterisks) primarily adjacent to the nasal epithelium (ne) as well as in the epithelia. Arrowheads indicate the epithelial seam. Scale bar = 100 μm.

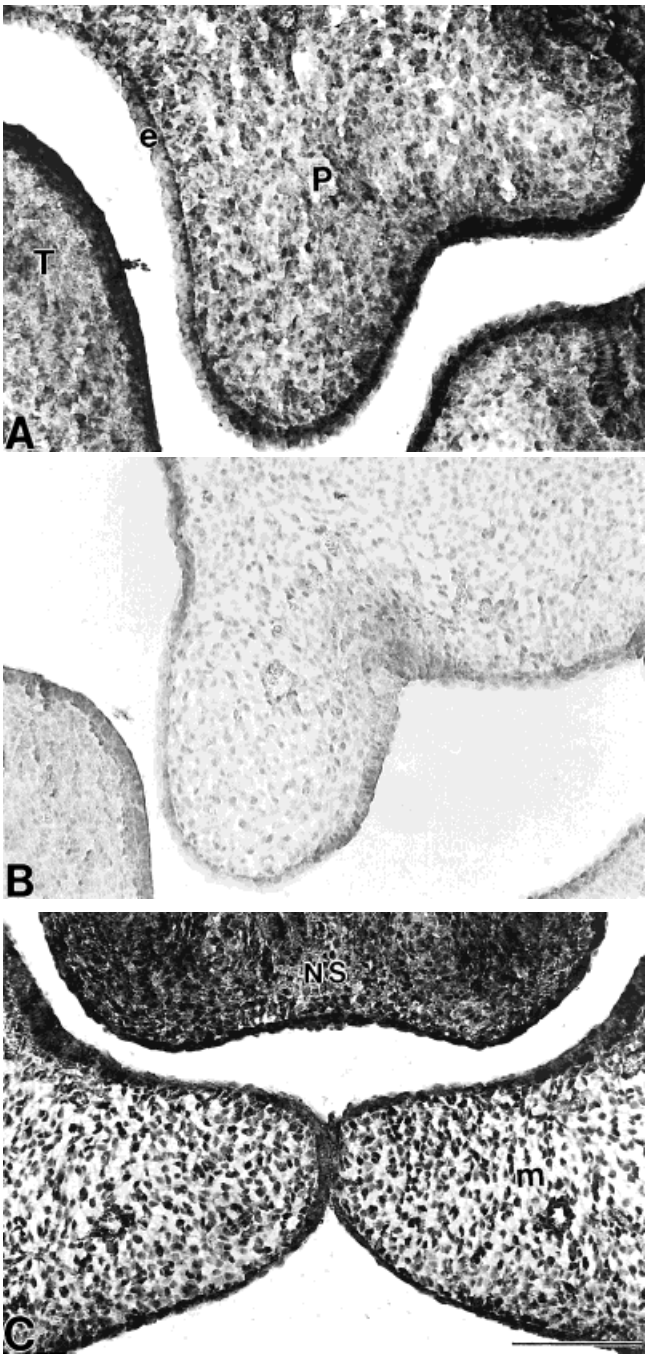

Fig. 6. Developmental expression of IGF-IIR mRNA by in situ hybridization in B10.A mouse palates. **A:** Vertical (E14) palatal shelves (P) hybridized with antisense probe. **B:** Negative control showing vertical (E14) palatal shelves hybridized with sense probe. **C:** Fusing (E15) palatal shelves. During palate development, IGF-IIR transcripts are expressed in the palatal epithelium (e) and throughout the mesenchyme (m). Note the positive signal in the tongue (T) and nasal septum (NS). Scale bar = 100 μm.

TGF-βs inhibit Cdk4 synthesis (Derynck, 1994). Because, in E14 B10.A embryonic palates, 1) IGF-IIR is up-regulated, 2) activated TGF-β2 is up-regulated, and 3) growth and development is significantly slower relative to its B10 congenic partner, we postulated that, whereas Cdk4 would be present in palatal tissue, *cdk*4 gene expression would be down-regulated in B10.A palates relative to B10. First, we determined by indirect immunofluorescence that Cdk4 protein is distributed throughout the mesenchyme and epithelium of developing palates (Fig. 11). Second, we quantitated Cdk4 mRNA transcripts in B10 and B10.A E14 palates (four or five litters/strain) by RNase protection assay

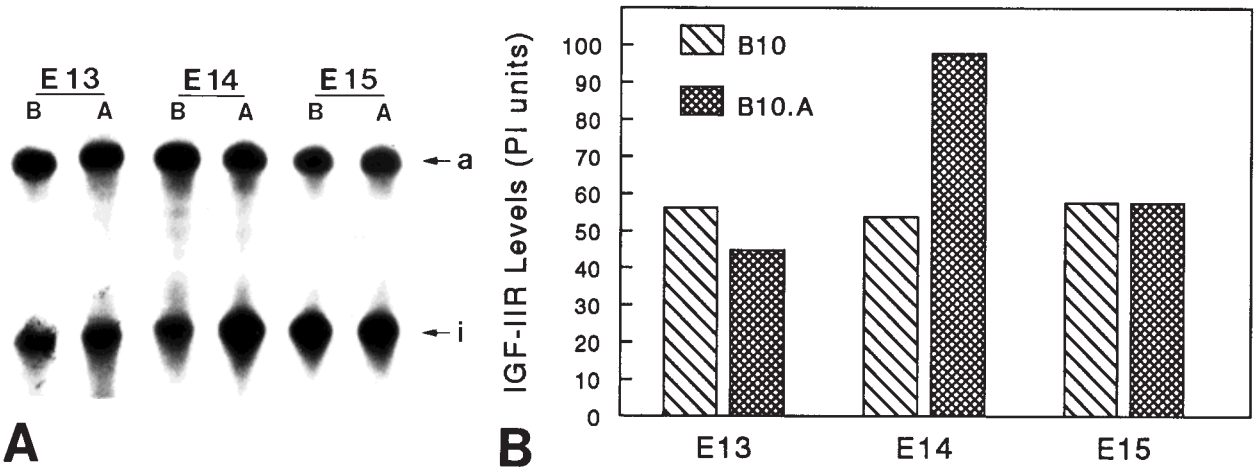

Fig. 7. IGF-IIR transcript levels in developing B10 and B10.A palates. **A:** An RNase protection assay was used to compare the steady-state levels of IGF-IIR mRNA in E13, E14, and E15 B10 (B) and B10.A (A) palates. Gels were quantified by phosphor image analysis, and IGF-IIR mRNA levels were normalized to β-actin expression in a given sample. i, IGF-IIR; a, β-actin. **B:** Bars represent mean phosphor imaging (PI) units and, with their 95% confidence limits, are as follows: 1) E13 B10: 56.23 (29.51–107.15); 2) E13 B10.A: 44.67 (28.18–112.20); 3) E14 B10: 53.70 (31.62–91.20); 4) E14 B10.A: 97.72 (69.18–138.04); 5) E15 B10: 57.54 (35.48–93.32); 6) E15 B10.A: 57.54 (31.62–104.71). E14 B10.A levels are 82% greater than E14 B10 ($P < 0.05$); all other mean levels are equivalent.

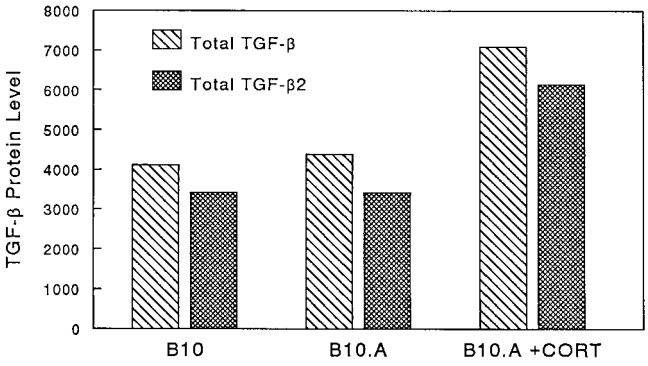

Fig. 8. Total transforming growth factor-β (TGF-β) and total TGF-β2 protein levels in E14 palates. Bars represent E14 mean counts and, with their 95% confidence limits, are as follows: 1) B10 total TGF-β: 4,110.09 (5,318.78–3,056.98); 2) B10 total TGF-β2: 3,419.91 (4,521.22–2,472.08); 3) B10.A total TGF-β: 4,385.09 (4,812.20–3,977.92); 4) B10.A total TGF-β2: 3,942.58 (4,312.55–3,589.21); 5) B10.A + corticosteroid (CORT) total TGF-β: 7,093.01 (10,528.81–4,333.59); 6) B10.A + CORT total TGF-β2: 6,138.72 (8,841.64–3,927.53). There is no substantial difference between strains in total TGF-β levels. CORT treatment induces a 62% increase in total TGF-β levels and a 56% increase in total TGF-β2 levels.

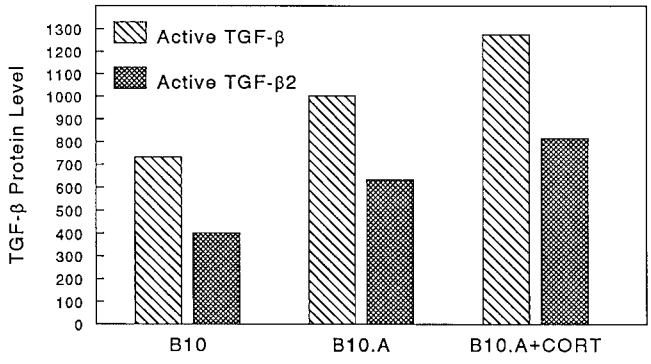

Fig. 9. Total active TGF-β and total active TGF-β2 protein levels in E14 palates. Bars represent E14 mean counts and, with their 95% confidence limits, are as follows: 1) B10 total active TGF-β: 731.70 (1,327.87–311.88); 2) B10 total active TGF-β2: 402.00 (811.11–135.02); 3) B10.A total active TGF-β: 999.82 (1,143.79–865.54); 4) B10.A total active TGF-β2: 632.02 (825.41–464.40); 5) B10.A + CORT total active TGF-β: 1,273.78 (1,828.42–819.10); 6) B10.A + CORT total active TGF-β2: 814.53 (1,175.80–519.38). B10.A palates exhibit a 37% greater level of active TGF-β than B10 and a 57% greater level of active TGF-β2. Elevated CORT levels significantly increase the levels of activated TGF-β, 64% of which is TGF-β2.

(Fig. 12). There was a 52% greater transcript level in B10 E14 palates than in B10.A palates ($t_7 = 3.42$; $P < 0.02$); this highly significant disparity is consistent with the smaller and slower growing palatal shelves and higher levels of activated TGF-β2 in B10.A embryos.

DISCUSSION

CP in humans is quite common (1 in 2,000 newborns), but its etiology and pathogenesis is obscure. We and others have produced a great deal of mammalian data in this regard but, alas, very little information about mechanism. The only hope we have of discriminating between what is signal and what is noise is to elucidate what details at the level of genetic circuits and contextual environments are essential to understanding more macroscopic regularities, normal or otherwise (Levin et al., 1997; Palsson, 1997; Strohman, 1997). Levin et al. (1997) posit that, "At each level [of organization], dynamics can be observed to emerge from the collective behaviors of individual units. The challenge, then, is to develop mechanistic models that begin from what is understood (or hypothesized) about the interactions of the individual units, and to use computation and analysis to explain emergent behavior [in nonlinear dynamical systems such as development] in terms of the statistical mechanics of ensembles of such units." We agree, and the present paper is our attempt at

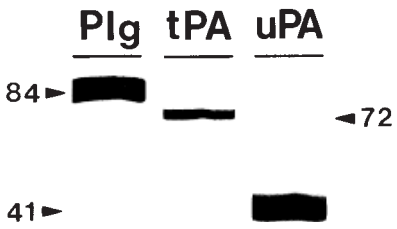

Fig. 10. Western blot demonstrating the presence of plasminogen (Plg), urokinase (uPA), and tissue plasminogen activator (tPA) in E14 B10.A palates. The M_r of Plg (84 kDa), tPA (72 kDa), and uPA (41 kDa) was calculated by using known molecular weight markers. The figure shown is a composite from three separate blots, each of which was incubated with a single antibody; the exposure time for each lane was optimized to demonstrate the presence of Plg, tPA, or uPA.

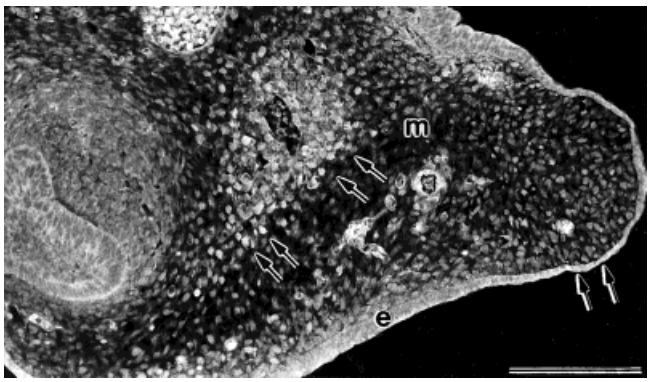

Fig. 11. Immunodetection of Cdk4 protein in the E14 B10.A mouse palate shows that Cdk4 protein (arrows) is detected throughout the mesenchyme (m) and epithelium (e). Scale bar = 100 μm

beginning this arduous journey. We take as our premise that, although morphogenesis obviously includes the genome, the former cannot be reduced to the latter without stumbling into a thoroughly perilous molecular form of genetic determinism (Strohman, 1997). Thus, we have chosen to investigate an epigenetic framework, the Fraser-Juriloff paradigm (Fig. 1).

IGF-IIR

Because B10 and B10.A mice are genetically identical, except for a 3–18 cM region of chromosome 17 (Vincek et al., 1990), we sought promising candidate genes encoded in this region that regulate embryonic growth. The best candidate is the gene for IGF-IIR mapped at approximately 8 cM from the centromere and 10 cM from the more telomeric H-2 (Lyon and Kirby, 1996). IGF-IIR is a large, membrane-bound glycoprotein (~300 kDa) that contains distinct binding sites for two ligands, IGF-II growth factor and mannose-6-phosphate (M6P) bearing molecules such as lysosomal enzymes and latent TGF-β (Jones and Clemmons, 1995; Vignon and Rochefort, 1992). This receptor does not appear to transduce mitogenic signals (Moats-Staat et al., 1995); instead, it sequesters IGF-II from type I IGF receptors, which mediate IGF-II growth signal transduction (Ballard et al., 1986; Lau et al., 1994; Wang et al., 1994; for reviews, see Barlow, 1995; Haig and Graham, 1991). This sequestration of IGF-II apparently fulfills the requirement for regulating the levels of ligand available for use in promoting growth (Barlow, 1995; Ellis et al., 1996; Filson et al., 1993). Critically, the *Igf*2r locus is genomically imprinted; primarily, the maternal copy is expressed in postimplantation embryos, giving rise to the widespread belief that imprinting serves to control embryonic growth in utero (Barlow, 1995; Barlow et al., 1991). Mouse embryos that inherit a nonfunctional maternal *Igf*2r reveal that the receptor is crucial for regulating normal embryonic growth and also for regulating the levels of free IGF-II ligand (Lau et al., 1994).

We have recently demonstrated that significant *Igf*2r gene transcriptional differences are strongly associated with differing rates of embryonic lung development in the B10/B10.A congenic mouse pair (Melnick et al., 1996). Here, we demonstrate 1) the spatiotemporal distribution of IGF-II, IGF-IR, and IGF-IIR protein and IGF-IIR mRNA with progressive palatogenesis (Figs. 3–6); and 2) that slower growing B10.A embryonic palates contain 82% more IGF-IIR transcript than faster growing B10 palates (Fig. 7). Our results are consistent with the conclusion that a significant elevation of IGF-IIR levels in B10.A embryonic palates reduces the concentration of IGF-II ligand available to the growth-promoting IGF-IR, resulting in a decreased growth rate of B10.A palates (Fig. 13). In terms of the Fraser-Juriloff paradigm (Fig. 1), this would place the B10.A genotype closer to the threshold than the B10 genotype; thus, exposure to even equivalent CORT-induced down-regulation of palatal growth results in far greater adverse phenotypic outcomes for B10.A than for B10 embryonic palates, as described by Melnick et al. (1981a).

The significant increase in B10.A IGF-IIR is transient and specific to E14, a day that is critical to mouse palatal growth. The most likely mechanism is a switch from mostly monoallelic expression of *Igf*2r to more biallelic expression, a switch that results from more than relaxation of methylation (Lerchner and Barlow, 1997). Lerchner and Barlow show that the paternal *Igf*2r allele is repressed in mice from E6.5 onward; however, a low level of paternal expression remains in tissues that highly express the maternal allele from E7.5 onward. Functional polymorphism (monoallelic/biallelic) exists with the parental imprinting of the human *IGF*2R gene as well (Xu et al., 1993). Lerchner and Barlow propose that mere DNA methylation is not sufficient to cause monoallelic expression and must occur by a multifactorial process (perhaps alternative promoter activation). This is supported by Smrzka et al. (1995), who found that the human *IGF*2R gene has the classic imprinting characteristics of monoparental methylation and replication asynchrony but does not show unequivocal monoallelic expression. Finally, additional genetic or epigenetic control of allelic expression is also supported by our matroclinus reciprocal hybrid cross data. B10.A.B10.A embryos had 60% greater IGF-IIR

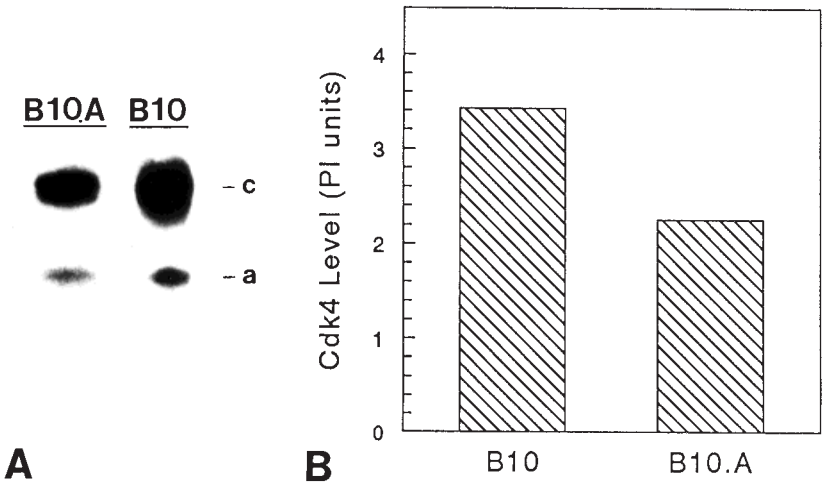

Fig. 12. Cdk4 mRNA levels in E14 B10 and B10.A palates. **A:** An RNase protection assay was used to compare the steady-state levels of Cdk4 mRNA in E14 B10 and B10.A palates. Three independent samples per strain were evaluated. Gels were quantified by phosphor image analysis, and Cdk4 mRNA levels were normalized to β-actin expression in a given sample. c, Cdk4; a, β-actin. **B:** Bars represent E14 palatal mean phosphor imaging units and, with their 95% confidence limits, are as follows: 1) B10: 3.42 (4.05–2.89); 2) B10.A: 2.25 (3.23–1.57). B10 palates exhibit a significant 52% increase in Cdk4 mRNA levels compared with B10.A palates.

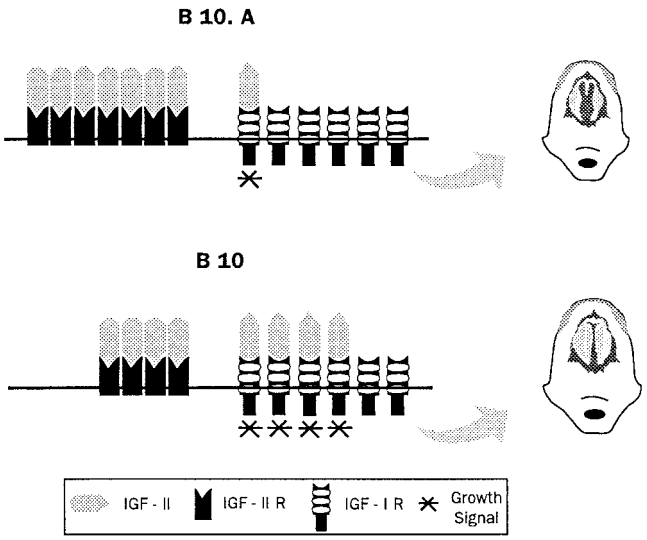

Fig. 13. Schematic of the IGF-IIR role in palate development. IGF-II binds to IGF-IR and IGF-IIR, having a higher affinity for IGF-IIR than for IGF-IR. The lower level of IGF-IIR in the E14 B10 palate results in increased availability of IGF-II, thereby enabling more of the ligand to bind the IGF-IR in B10 palates compared with B10.A palates. Because only IGF-II/IGF-IR transduces a mitogenic signal (asterisks), the result is an accelerated rate of morphogenesis in the B10 palate compared with the B10.A palate.

levels ($P < 0.01$) than B10.A.B10 embryos, which, in turn, were equivalent to B10.B10.A and B10.B10 embryos. This can only occur if the control of monoallelic expression is both biparental and B10-dominant.

Latent and Active TGF-βs

The TGF-β family of autocrine/paracrine growth factors participates in regulating cell proliferation and differentiation and extracellular matrix formation and degradation (Derynck, 1994; Lawrence, 1996). TGF-βs are present in the developing palate (Linask et al., 1991; Pelton et al., 1990); TGF-β1 and TGF-β3 are localized primarily in the epithelium, whereas TGF-β2 is expressed primarily in the mesenchyme, the principal site of palatal process growth (Jaskoll et al., 1996a). TGF-β2 is known to inhibit palatal cell proliferation (Ferguson, 1988). The level of TGF-β2 mRNA significantly decreases with progressive palatal development; this down-regulation in TGF-β2 expression is associated with increased mesenchymal cell proliferation and palatal shelf growth (Jaskoll et al., 1996a).

All three mammalian TGF-βs are 25-kD homodimers in their biologically active form; they show a high level of sequence conservation (Lawrence, 1996). The larger, latent TGF-β is composed of one mature TGF-β molecule noncovalently bound to the proregion dimer, the latency-associated peptide (LAP); TGF-β1 and TGF-β2 LAPs contain M6P residues (Brunner et al., 1992; Dennis and Rifkin, 1991; Gleizes et al., 1997). Cellular activation of latent TGF-β appears to require binding to the M6P binding site of the IGF-IIR and is plasmin and plasminogen activator-dependent (Dennis and Rifkin, 1991; Gleizes et al., 1997). Plasminogen and plasminogen activators are all found in the embryonic palate (Fig. 10). It is probably more than a coincidence that the polymorphic plasminogen gene, *Plg*, is closely linked to *Igf*2r (Barlow et al., 1991; Friezner Degen et al., 1990).

The relationship between TGF-β2 activation and IGF-IIR seems to us to be a key one. Because E14 is a critical stage of palatal growth that is dependent on the down-regulation of TGF-β2 (Jaskoll et al., 1996a), and known strain differences in growth rate (Melnick and Jaskoll, 1992) are associated with TGF-β2 (Jaskoll et al., 1996a) and IGF-IIR (present study) expression, it

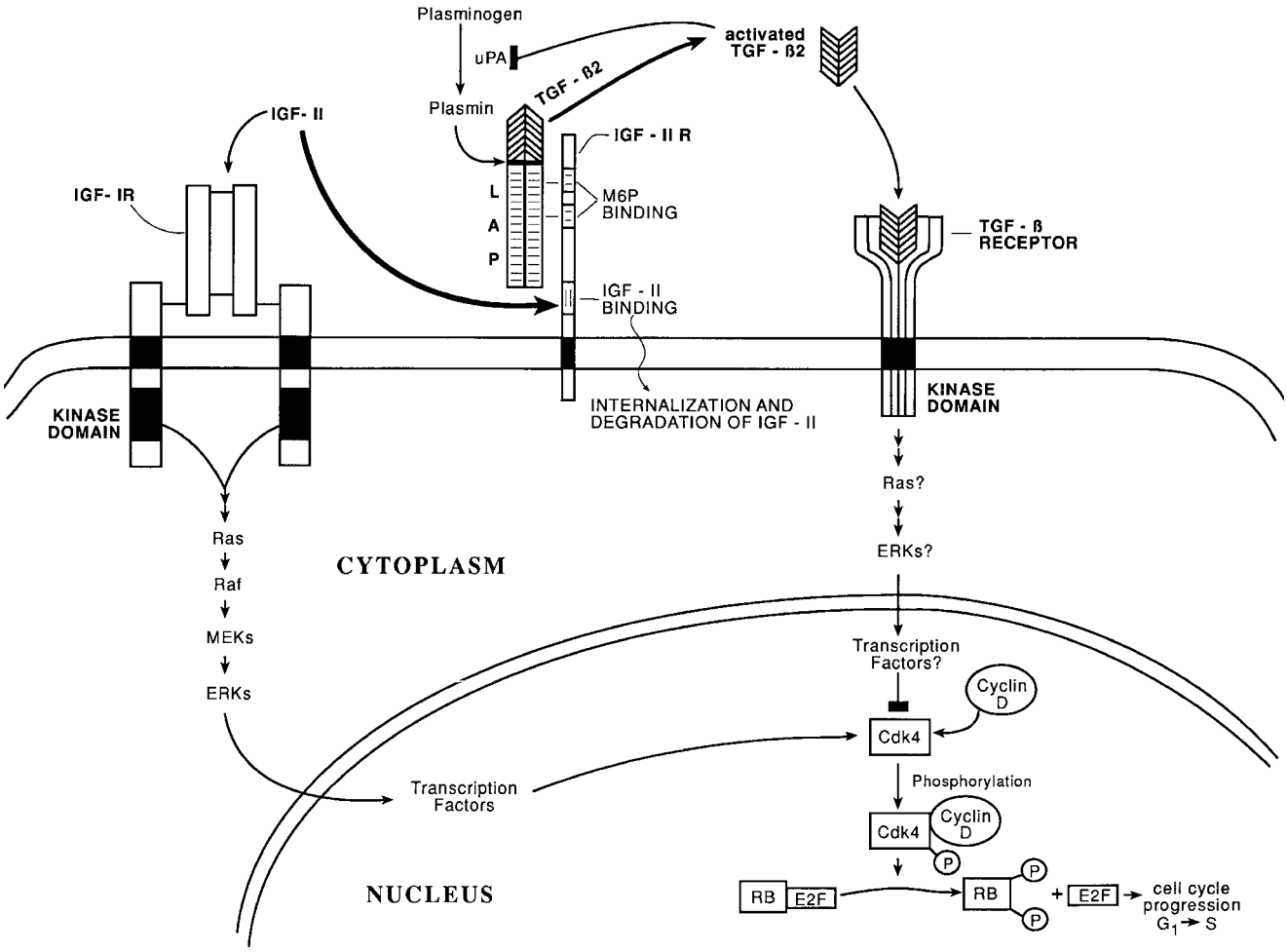

Fig. 14. Epigenetic model of information processing related to cell proliferation. The model is based on study data and literature cited in the text. IGF, insulin-like growth factor; R, receptor; TGF-β, transforming growth factor-beta; LAP, latency-associated protein; M6P, mannose-6-phosphate; uPA, urokinase-type plasminogen activator; MEK, mitogen-activated protein kinase kinase; ERK, mitogen-activated protein kinase; Cdk, cyclin-dependent protein kinase; RB, retinoblastoma protein; E2F, a family of transcription factors. For details, see text.

was reasonable to hypothesize that greater availability of the IGF-IIR receptor in B10.A embryonic palates would result in a higher level of activated TGF-β2. Approximately one-fifth of the total TGF-β is activated, and approximately two-thirds of the total activated TGF-β is TGF-β2 (Figs. 8, 9). This is consistent with recent findings in embryonic hearts, which show that active TGF-β has a very limited and specific distribution, whereas latent TGF-β is far more widespread and abundant (Ghosh and Brauer, 1996). What is particularly noteworthy is that E14 B10.A embryonic palates have a 57% greater level of active TGF-β2 than B10 embryonic palates (Fig. 9), even though their total TGF-β2 levels are nearly identical (Fig. 8). This is precisely what we expected: more IGF-IIR receptor, more active TGF-β2.

TGF-β signalling is effected through a set of transmembrane Ser/Thr kinase receptors (Derynck, 1994). Palatal mesenchymal cells contain all known TGF-β receptors (Linask et al., 1991). TGF-β-induced inhibition of cell proliferation is related to arrest of the G_1-S transition of the cell cycle through a down-regulation of Cdk4 and, perhaps, other G_1 factors, like cyclin E and Cdk2 (Derynck, 1994). Thus, one would expect an inverse relationship between the levels of active TGF-β2 and Cdk4. Indeed, there was: B10 embryonic palates with a lower level of active TGF-β2 had a 52% greater level of Cdk4 transcript than B10.A with a higher level of active TGF-β2. Thus, the variation of TGF-β2/IGF-IIR-mediated growth inhibition in the late G_1 phase of the cell cycle would appear to account for the slower growth and development of B10.A embryonic palates relative to its B10 congenic partner.

IGF-IIR/TGF-β2 Epigenetic Model

Figure 14 is an epigenetic model of information processing as it relates to cell proliferation; it is based on the present studies and the cited literature. Epigenetic networks are nonlinear, complex, and adaptive systems that include feedback to the genome and

changing patterns of gene expression (Strohman, 1997). Although the complex molecular mechanism of cell proliferation control (Fig. 14) is not strictly reducible to its parts (Fig. 14, labelled boxes, ovals, and arrows), some of the known factors that make this complex epigenetic network nonlinear and adaptive include the following: 1) IGF-IIR binds IGF-II with a very significantly greater affinity than IGF-IR (Jones and Clemmons, 1995). 2) Although ligand binding of the IGF-IR is not a sine qua non for cell cycle progression, it is probably required for the cell cycle to be maintained at a normal rate (LeRoith et al., 1995). 3) Since IGF-II and M6P-bearing molecules (e.g., latent TGF-β2) competitively bind to their cognate IGF-IIR sites because of steric hinderance or conformational change, any imbalance in ligand(s) and receptor concentration is likely to alter associated biological functions, such as IGF-II degradation, IGF-II/IGF-IR binding, and TGF-β2 binding and activation (Vignon and Rochefort, 1992). 4) TGF-β decreases the mRNA expression of both uPA and tPA plasminogen activators and may stimulate PA-inhibitor production (Agrawal and Brauer, 1996; Keski-Oja et al., 1988). 5) Plasmin-dependent activation of TGF-β is modulated by surface localization of uPA by its receptor (Odekon et al., 1994). This, then, is a dynamical network that uses a continuous logic to learn its rules from changing conditions.

CORT-Induced Palate Dysmorphogenesis

It is well established that CORT induces CP manyfold in B10.A embryos relative to its B10 congenic partner when injected on E12 into pregnant dams at physiological levels (Melnick et al., 1981a). CORT treatment has been shown to inhibit palatal mesenchymal cell proliferation, resulting in smaller palatal processes and CP (Potchinsky et al., 1996; Salomon and Pratt, 1979). CORT also delays by 1 day the down-regulation of palatal TGF-β2 transcription normally seen on day 14 of gestation (Jaskoll et al., 1996a). We report here that, in E14 B10.A palates, elevated CORT exposure in utero significantly increases TGF-β protein levels, 87% of which is TGF-β2, as well as the levels of active TGF-β, 64% of which is TGF-β2. This would enhance the TGF-β2/IGF-IIR-mediated growth inhibition via down-regulation of Cdk4 in late G_1 of the cell cycle. In terms of the Fraser-Juriloff paradigm (Fig. 1), B10.A embryos that are already close to the threshold of abnormality would be pushed beyond that threshold with the CORT-induced up-regulation of active TGF-β2. Thus, we have an outline of the *pathogenetic mechanism* in B10.A embryos: Slower growing B10.A embryos have an up-regulation of IGF-IIR that serves to sequester IGF-II from the growth-promoting IGF-IR and to bind more CORT-up-regulated, latent TGF-β2 for subsequent plasmin-dependent activation. Higher levels of TGF-β2 signaling lead to palatal growth inhibition at a critical stage of palatogenesis and, thus, subsequent CP.

Mouse/Human Correlation

Mouse models of human dysmorphogenesis have limited utility unless they are reasonably congruous with respect to disease phenotype, etiology, and pathogenesis. Although it is known that cortisone and various analogs cause CP in mice when administered at human-equivalent doses (Pinsky and DiGeorge, 1965; Walker, 1965), there is scant evidence to support teratogenicity in humans (Fraser and Sajoo, 1995). However, even if direct CORT-induced CP is rarely seen in humans, other known (or highly suspect) inducers of human CP also elevate maternal plasma CORT levels in mammals. These drugs include phenytoin (Hansen et al., 1988; Hanson and Smith, 1975), diazepam (Barlow et al., 1980; Safra and Oakley, 1975), smoking (Andrews and McGarry, 1972; Hwang et al., 1995; Lieberman et al., 1992), and probably others yet unknown. In addition, stress-induced up-regulation of maternal CORT may act alone or synergistically with other factors to increase CP incidence (Rasco and Hood, 1995; Rosenzweig and Blaustein, 1970). Thus, a common CORT-modulated pathway, such as the one discussed above, would account for the pathogenetic mechanism of apparently disparate human teratogens.

One may reasonably suppose that most, if not all, CPs in a given population have a similar genetic cause, but penetrance (manifestation) is quite low, because the environmental exposure frequency is low; even with a strong gene-environment interaction, the recurrence risk would be low. Assuming recessive inheritance of a "susceptibility genotype" and using the relationships derived by Penrose (1953) and Khoury et al. (1988) and the frequency of CP in the general population and siblings of probands (Shields et al., 1981), one would arrive at a genotype frequency (q) of 0.064 and a trait manifestation of 12%. Manifestation would depend on exposure to specific environmental factors, and approximately one in every eight persons would be a susceptibility genotype carrier (homozygous or heterozygous). These calculations serve to explain the relatively high frequency of CP in humans (~1/2,000) and the relatively low number of families with multiple affected persons. However, they provide no clue to the nature of the susceptibility genotype.

Christiansen and Mitchell (1996) argue convincingly that two or three loci are probably related to susceptibility; this has been known for two decades in *inbred* mouse strains (Biddle and Fraser, 1977). Perhaps the most relevant model from the perspectives of both embryology and genetics is "emergenic" inheritance, or emergenesis (Li, 1987). An emergenic trait is one that is determined by a particular combination of alleles at a number of gene loci, a so-called gene constellation. When any one allele is absent, it destroys the constellation, and the emergenic trait disappears. Meiosis in *outbred* populations will ensure that any constellation will not be preserved as such. Thus, an emergenic trait will usually not be Mendelian, even though the pheno-

type itself is genetically determined. Emergenesis is particularly interesting as a model, because it allows us to consider together the multigenic correlates of a given embryologic process, e.g., mesenchymal cell proliferation in palatogenesis. Based on our present studies, these multigenic correlates may include the *Igf*2r gene (and/or a cognate regulatory gene) and the polymorphic *Plg* gene, which demonstrates allelic differences between the B10 strain and the A strain used to derive the B10.A congenic partner (Friezner Degen et al., 1990). It is also likely to include at least one other closely linked gene related to TGF-β activation on mouse chromosome 17 and human chromosome 6. These would then comprise the *Igf*2r-*Plg*-*"X"* gene constellation, and the emergenic trait would be decreased mesenchymal cell proliferation.

If emergenesis is truly the case, then human linkage studies are likely to remain unproductive (Christiansen and Mitchell, 1996; Melnick, 1992). In essence, CP is both a complex trait and not the relevant phenotype. A more germane phenotype, such as mesenchymal cell proliferation, is also a complex trait and is not unlike a quantitative trait (see, e.g., Fig. 1). The only extant methods for mapping emergenic trait loci are not applicable to humans, because they depend on carefully constructed breeding studies (Lander and Botstein, 1989). Identification of emergenic trait loci using genetically defined mice, epigenetic developmental paradigms, and novel, nonlinear computational methodologies will nevertheless permit an informed search for human homologs.

EXPERIMENTAL PROCEDURES

Animal Mating and Tissue Collection

B10.A/SgSn (B10.A, H-2^a) and C57BL/10SgSn (B10, H-2^b) mice were purchased from Jackson Laboratories (Bar Harbor, ME) and maintained in our animal facilities in accordance with National Institutes of Health Guidelines. Animals were mated overnight, and females were examined for vaginal plugs the next morning; this day was considered day 0 of gestation. Dams were anesthetized with metafane and killed by cervical dislocation on the appropriate day of gestation. All embryos were staged according to Theiler (1989). Palatal shelves were dissected from staged embryos on days E13, E14, or E15 of gestation, pooled by litter, and stored at −70°C. E12.5 to E15 heads were fixed for immunohistochemistry or in situ hybridization as described below. In a second series of experiments, B10, B10.A, B10.A.B10, and B10.B10.A embryos were generated, and E14 palatal shelves from five or six litters/cross were collected for RNase protection assays.

In CORT-treated experiments, pregnant B10.A mice were injected with 6 mg/kg body weight triamcinolone hexacetonide (Aristospan; Fujisawa Pharmaceutical Co., Deerfield, IL) or were sham injected at 9 A.M. on E12. This steroid treatment results in 94% of the embryos being affected, as determined by the presence of CP (Jaskoll et al., 1996a). To assay TGF-β activity, sham-injected control and CORT-treated E14 palatal shelves were dissected and cultured as described below.

Analysis of IGF-IIR and Cdk4 Transcripts by Ribonuclease Protection Assay

Steady-state levels of IGF-IIR and Cdk4 transcripts were measured with an RNase protection assay essentially as described in Melnick et al. (1996). Each independent sample was a pool of five to eight palates from one litter; a minimum of four independent samples per strain per experiment were assayed. Each sample was assayed two to three times and quantitated by phosphor image analysis with ImageQuant software and background correction (Molecular Dynamics, Sunnyvale, CA). The control without palatal RNA contained 50 μg yeast tRNA. β-actin transcripts provided an internal standard for each sample. A 165-nt IGF-IIR protected fragment, a 295-nt Cdk4 protected fragment, and a 250-nt β-actin protected fragment are detected. Protected RNAs corresponding to hybrids between IGF-IIR probe or Cdk4 probe and its target mRNAs were quantitated by phosphor image analysis (Molecular Dynamics) and normalized to the amount of protected β-actin probe present in each sample. Ratios were mathematically transformed to meet the analytical assumptions of normality and homoscedasticity, means were calculated, and differences between mean ratios were compared by t test (Sokal and Rohlf, 1981).

Probes for RNase Protection Assays

A plasmid containing a 164-base pair (bp) mouse cDNA IGF-IIR fragment insert corresponding to mouse exon 11 was obtained from Dr. Peter Rotwein (Szebenyi and Rotwein, 1994). The plasmid was subcloned into pBluescript. The purified plasmid was linearized with *Eco*RI, and a ^{32}P-labelled antisense probe was generated by using T3 RNA polymerase and ^{32}P-UTP (ICN, Costa Mesa, CA). A plasmid containing a 1.2-kb mouse cDNA corresponding to the entire coding region of mouse *cdk*4 (cdk4/PSK-J3) was obtained from Dr. Charles J. Sherr (Matsushime et al., 1992), linearized with *Pst*I, and an ^{32}P-labelled antisense probe was generated by using T7 RNA polymerase. A linearized, gel-purified plasmid containing a 250-bp mouse β-actin cDNA insert was purchased from Ambion (Austin, TX), linearized with *Eco*RI, and used to produce a ^{32}P-labelled antisense probe using T7 RNA polymerase.

In Situ Hybridization

The spatial distribution of IGF-IIR transcripts was determined by in situ hybridization. Mouse embryonic heads were fixed overnight in 4% paraformaldehyde in phosphate-buffered saline (PBS) at 4°C, dehydrated through graded ethanol concentrations and xylene, and embedded in paraplast. Sections of 8 μm were cut and mounted on slides coated with 3-trithoxy-silylpropylamine. In situ hybridization was performed by using digoxigenin (DIG)-labelled IGF-IIR riboprobes as de-

scribed previously (Melnick et al., 1996). Controls consisted of 1) sections hybridized with sense RNA probes and 2) sections pretreated with RNase prior to hybridization with the antisense RNA probe. No hybridization signal was detected in control sections. In situ hybridization was performed on a minimum of eight sections with sense and antisense probes from three to five different embryos as well as with RNase-pretreated controls.

IGF-IIR, IGF-IR, IGF-II, and Cdk4 Immunolocalization

Three litters of B10.A and B10 mouse heads were collected on each of day of gestation from day 12.5 to day 15.0, fixed at 4°C in Carnoy's fixative, processed, and sectioned as described previously (Melnick et al., 1996). Sections were incubated overnight at room temperature (RT) with antirat IGF-IIR antiserum (1:50), antimouse Cdk4 antibody (1:10), or antihuman IGF-IRα antibody (1:20). The sections were then incubated sequentially with biotin-labelled goat antirabbit immunoglobulin (IgG; 1:100) and fluorescein isothiocyanate (FITC)-labelled streptavidin (1:100). Because a monoclonal anti-IGF-II antibody was used, it was necessary to block nonspecific cross reactivity with endogenous IgG in the mouse palate by preincubating the sections with unlabelled rabbit antimouse IgG (1:2) for 1 hr at 37°C, and incubating overnight at RT with antirat IGF-II antibody (1:20). The sections were then incubated sequentially with biotin-labelled rabbit antimouse IgG (1:100) and FITC-labeled streptavidin (1:100). The slides were examined with a Zeiss Epifluorescence Photomicroscope (Thornwood, NY) and photographed by using TMAX 400 film at constant exposure. Control sections were incubated in the absence of primary antibodies; controls were routinely negative (data not shown). Three to six heads per strain per antibody were evaluated for each day of gestation.

Antibodies

Antirat IGF-IIR antiserum was generously provided by Dr. Peter Nissley; its characterization, specificity, and cross-reactivity with mouse IGF-IIR has been demonstrated previously (Melnick et al., 1996; Sklar et al., 1989). Antimouse Cdk4 antibody was purchased from Santa Cruz Biotech, Inc. (Santa Cruz, CA). Antihuman IGF-IRα antibody was purchased from Santa Cruz Biotech, Inc. IGF-IRα polyclonal antibody was made against an epitope corresponding to amino acids 31–50 mapping at the amino terminus of the precursor form of human IGF-IRα, a sequence that is identical to the corresponding mouse sequence. This antibody has been shown by Santa Cruz Biotechnology to react with the IGF-IRα chain in mouse, rat, and human by Western blotting and immunohistochemistry. Antirat IGF-II monoclonal antibody was purchased from Amano Enzyme USA Co. (Troy, VA); this antibody has been used to identify rat and mouse IGF-II (Tanaka et al., 1989; Zhan et al., 1994). Unlabelled rabbit antimouse IgG and biotin-labelled goat antirabbit and rabbit antimouse IgGs were purchased from Organon Teknika (Malvern, PA); FITC-labelled streptavidin was purchased from Zymed (South San Francisco, CA).

Western Blot Analysis

To demonstrate the presence of Plg, tPA, and uPA in embryonic mouse palates, Western blot analyses were conducted. Four litters of E14 B10.A palatal shelves were collected and stored at −70°C. The tissues were extracted, equivalent amounts of total protein were fractionated by sodium dodecyl sulfate-polyacrylamide gel electrophoresis, and immunoblotted essentially as described previously (Jaskoll et al., 1996b). Blots were incubated overnight at 4°C with anti-tPA antibody (1:50), anti-uPA antibody (1:100), or anti-Plg antibody (1:50). The following day, the blots were incubated in alkaline phosphatase-conjugated antirabbit IgG (1:1,000). The molecular weight of proteins was calculated by using known molecular weight markers (BioRad, Richmond, CA). The controls consisted of blots incubated in the absence of primary antibodies; controls were routinely negative (data not shown). A minimum of three independent samples were analyzed in duplicate for each antibody.

Antibodies

Antimouse tPA and antimouse uPA antibodies were purchased from American Diagnostic Inc. (Greenwich, CT); antihuman Plg antibody was purchased from Accurate Chemicals (Westbury, NY). Alkaline phosphatase-conjugated antirabbit IgG antibody was purchased from Pierce Scientific (Rockford, IL). To demonstrate the cross-reactivity of antihuman Plg antibodies with mouse Plg, we first evaluated adult mouse liver with Western blot by using three different antihuman Plg antibodies, because liver is the site of highest Plg production. All three antibodies detected the reported 84-kDa band; the antibody used in subsequent experiments was the one that showed the greatest recognition.

Assay for TGF-β Activity

TGF-β was collected in conditioned medium according to the method of Barcellos-Hoff et al. (1994); this method does not activate latent TGF-β. Palatal shelves were dissected by litter from E14 B10, B10.A, and CORT-treated B10.A; chopped; and incubated for 1 hr with agitation at 37°C in Dulbecco's minimal essential medium (DMEM)/F12 media (40-µl medium/palatal shelf; Sigma Chemical Co., St. Louis, MO) containing 2% bovine serum albumin (BSA). To each ml of conditioned medium, 2.5 µl of 0.2 M phenylmethysulfonyl fluoride (Sigma Chemical Co.) and 5 µl of aprotinin (Sigma Chemical Co.) were added. The conditioned medium was immediately frozen on dry ice and stored at −70°C.

TGF-β activity was measured by using the PAI-1 luciferase assay in mink epithelial cells stably trans-

fected with an expression construct containing a truncated PAI-1 promotor fused to a firefly luciferase reporter gene. Addition of active TGF-β to these cells results in a dose-dependent expression of luciferase (Abe et al., 1994). Reporter mink cells were plated in 96-well plates, 1.6×10^4 cells/well in DMEM/F12 (Sigma Chemical Co.) with 10% fetal calf serum (FCS) and were allowed to attach for 3 hr or more. The serum containing medium was then removed and replaced with palatal extracts diluted with DMEM/F12 containing 0.1% BSA in parallel with TGF-β standards diluted in the same medium. After 16–18 hr of incubation, the cells were washed, lysed, and assayed for luciferase activity by using a luciferase kit (Analytical Luminescence Laboratory, Ann Arbor, MI). Light emitted from cell lysates incubated at RT with luciferin substrate was measured by using a scintillation counter equipped with a single photon monitor. Samples were assayed in duplicate at two dilutions. To confirm the specificity of the method, each plate extract was incubated at RT with a pan-TGF-β neutralizing antibody (Genzyme, Cambridge, MA) before analysis; there was negligible TGF-β detected in neutralized samples. Total TGF-β (active + latent) was measured after heating the extracts at 80°C for 5 min to activate any latent TGF-β. TGF-β2 was measured by incubating the palatal extracts (active TGF-β2) or heated extracts (total TGF-β2) for 2 hr at RT with an excess of TGF-β2 neutralizing antibody (R and D Systems, Minneapolis, MN) and comparing TGF-β levels in the neutralized samples with the untreated samples. Independent assays were performed on five litters of E14 palates (five to ten embryos/litter) for each group: B10, B10.A, and CORT-treated B10.A. The data were appropriately transformed to satisfy the assumptions of parametric hypothesis testing and were analyzed as described above.

ACKNOWLEDGMENTS

We thank Dr. Peter Nissley for his generous gift of IGF-IIR antiserum, Dr. Peter Rotwein for his generous gift of *Igf*2r probe, Dr. Charles Sherr for his generous gift of *cdk*4 probe, Dr. Daniel Rifkin for his generous gift of reporter cells, Dr. Myron Goodman for use of his phosphor imager, and Dr. Yan-Min Zhou for technical assistance.

REFERENCES

Abe M, Harpel JG, Metz CN, Koskatoff DL, Rifkin DB. An assay for transforming growth factor β using cells transfected with a plasminogen activator-1 promotor-luciferase construct. Anal. Biochem. 1994; 216:276–284.

Agrawal M, Brauer PR. Urokinase-type plasminogen activator regulates cranial neural crest cell migration in vitro. Dev. Dyn. 1996;207: 281–290.

Andrews J, McGarry JM. A community study of smoking in pregnancy. J. Obstet. Gynecol. Br. Commonweal. 1972;79:1057–1073.

Ballard FJ, Read LC, Francis GL, Bagley CJ, Wallace JC. Binding properties and biological potencies of insulin-like growth factors in L6 myoblasts. Biochem. J. 1986;233:223–230.

Barcellos-Hoff MH, Derynck R, Tsang LS, Weatherbee JA. Transforming growth factor β activation in irradiated murine mammary gland. J. Clin. Invest. 1994;93:892–899.

Barlow DP. Gametic imprinting in mammals. Science 1995;270:1610–1613.

Barlow DP, Stoger R, Herrman BG, Saito K, Schweifer N. The mouse insulin-like growth factor type 2 receptor is imprinted and closely linked to the *Tme* locus. Nature 1991;349:84–87.

Barlow SM, Knight AF, Sullivan FM. Diazepam-induced cleft palate in the mouse: The role of endogenous maternal corticosterone. Teratology 1980;21:149–155.

Biddle FG, Fraser FC. Cortisone-induced cleft palate in the mouse. A search for the genetic control of the embryonic response trait. Genetics 1977;85:289–302.

Bonner JJ, Slavkin HC. Cleft palate susceptibility linked to histocompatibility-2 (H-2) in the mouse. Immunogenetics 1975;2:213–218.

Brunner AM, Lioubin MN, Marquardt H, Malacko AR, Wang WC, Shapiro RA, Neubauer M, Cook J, Madisen L, Purchio AF. Site-directed mutagenesis of glycosylation sites in the transforming growth factor-β1 (TGFβ1) and TGFβ2 (414) precursors and of cysteine residues within mature TGFβ1: Effects on secretion and bioactivity. Mol. Endocrinol. 1992;6:1691–1700.

Carroll PM, Tsirka SE, Richards WG, Frohman MA, Strickland S. The mouse tissue plasminogen activator gene 5′ flanking region directs appropriate expression in development and a seizure-enhanced response in the CNS. Development 1994;120:3173–3183.

Christiansen K, Mitchell LE. Familial recurrence-pattern analysis of nonsyndromic isolated cleft palate—A Danish registry study. Am. J. Hum. Genet. 1996;58:182–190.

Dennis PA, Rifkin DB. Cellular activation of latent transforming growth factor β requires binding to the cation-independent mannose 6-phosphate/insulin-like growth factor type II receptor. Proc. Natl. Acad. Sci. USA 1991;88:580–584.

Derynck R. TGF-β-receptor mediated signaling. Trends Biochem. Sci. 1994;19:548–553.

Ellis MJC, Leav BA, Yang Z, Rasmussen A, Pearce A, Zweibel JA, Lippman ME, Cullen KJ. Affinity for the insulin-like growth factor-II (IGF-II) receptor inhibits autocrine IGF-II activity in MCF-7 breast cancer cells. Mol. Endocrinol. 1996;10:286–297.

Ferguson MWJ. Palate development. Development 1988;103:41–60.

Filson AJ, Louvi A, Efstratiadis A, Robertson EJ. Rescue of the T-associated maternal effect in mice carrying null mutations of *Igf*-2 and *Igf* 2r, two reciprocally imprinted genes. Development 1993;118: 731–736.

Fraser FC. Animal models for craniofacial disorders. In: Melnick M, Bixler D, Shields ED, eds. Etiology of Cleft Lip and Cleft Palate. New York: Alan R. Liss, Inc., 1980:1–23.

Fraser FC, Fainstat TD. Production of congenital defects in the offspring of pregnant mice treated with cortisone. Pediatrics 1951;8: 527–533.

Fraser FC, Sajoo A. Teratogenic potentials of corticosteroids in humans. Teratology 1995;51:45–46.

Friezner Degen SJ, Bell SM, Schaefer LA, Elliott RW. Characterization of the cDNA coding for mouse plasminogen and localization of the gene to mouse chromosome 17. Genomics 1990;8:49–61.

Gasser DL, Goldner-Sauve A, Katsumata M, Goldman AS. Restriction fragment length polymorphisms, glucocorticoid receptors and phenytoin-induced cleft palate in congenic strains with steroid susceptibility. J. Craniofac. Genet. Dev. Biol. 1991;11:366–371.

Ghosh S, Brauer PR. Latent transforming growth factor-β is present in the extracellular matrix of embryonic hearts in situ. Dev. Dyn. 1996;205:126–134.

Gleizes P-E, Munger JS, Nunes I, Harpel JG, Mazzieri R, Noguera I, Rifkin DB. TGF-β latency: Biological significance and mechanisms of activation. Stem Cells 1997;15:190–197.

Goldman AS. Biochemical mechanism of glucocorticoid- and phenytoin-induced cleft palate. In: Zimmerman EF, ed. Current Topics in Developmental Biology. New York: Academic Press, 1984:217–239.

Good L, Jaskoll T, Melnick M, Minkin C. The major histocompatibility complex and murine fetal development. J. Dent. Res. 1991;70:579.

Häckel C, Radig K, Röse I, Roessner A. The urokinase plasminogen activator (uPA) and its inhibitor (PAI-1) in embryo-fetal bone formation in the human: An immunohistochemical study. Anat. Embryol. 1995;192:363–368.

Haig D, Graham C. Genomic imprinting and the strange case of the insulin-like growth factor II receptor. Cell 1991;64:1045–1046.
Hansen DK, Holson RR, Sullivan PA, Grafton TF. Alterations in maternal plasma corticosterone levels following treatment with phenytoin. Toxicol. Appl. Pharmacol. 1988;96:24–32.
Hanson JW, Smith DW. The fetal hydantoin syndrome. J. Pediatr. 1975;87:285–291.
Hu CC, Jaskoll T, Minkin C, Melnick M. The mouse major histocompatibility complex (H-2) and fetal lung development: Implications for human pulmonary maturation. Am. J. Med. Genet. 1990;35:126–131.
Hwang SJ, Beaty TH, Panny SR, Street NA, Joseph JM, Gordon S, Mcintosh I, Francomano CA. Association study of TGF-alpha TAQ1 polymorphism and oral clefts-indication of gene-environment interaction in population-based sample of infants with birth defects. Am. J. Epidemiol. 1995;141:629–636.
Jaskoll T, Hu CC, Melnick M. Mouse major histocompatibility complex and lung development: Haplotype variation, H-2 immunolocalization and progressive maturation. Am. J. Med. Genet. 1991;39:422–436.
Jaskoll T, Choy HA, Chen H, Melnick M. Developmental expression and CORT-regulation of TGF-β and EGF receptor mRNA during mouse palatal morphogenesis: Correlation between CORT-induced cleft palate and TGF-β2 mRNA expression. Teratology 1996a;54: 34–44.
Jaskoll T, Choy HA, Melnick M. The glucocorticoid-glucocorticoid receptor signal transduction pathway, transforming growth factor-β, and embryonic mouse lung development in vivo. Pediatr. Res. 1996b;39:749–759.
Jones JI, Clemmons DR. Insulin-like growth factors and their binding proteins: Biological actions. Endocrine Rev. 1995;16:3–34.
Keski-Oja J, Blasi F, Leof EB, Moses HL. Regulation of the synthesis and activity of urokinase plasminogen activator in A549 human lung carcinoma cells by transforming growth factor-β. J. Cell Biol. 1988;106:451–459.
Khoury MJ, Flanders WD, Beaty TH. Penetrance in the presence of genetic susceptibility to environmental factors. Am. J. Med. Genet. 1988;29:397–403.
Landers ES, Botstein D. Mapping Mendelian factors underlying quantitative traits using RFLP linkage maps. Genetics 1989;121: 185–199.
Lau M, Stewart CEH, Liu Z, Bhatt H, Rotwein P, Stewart CL. Loss of imprinted IGF2/cation-independent mannose-6-phosphate receptor results in fetal overgrowth and perinatal lethality. Genes Dev. 1994;8:2953–2963.
Lawrence DA. Transforming growth factor-β: A general review. Eur. Cytokine Netw. 1996;7:363–374.
Lerchner W, Barlow DP. Paternal repression of the imprinted mouse *Igf*2r locus occurs during implantation and is stable in all tissues of the postimplantation mouse embryo. Mech. Dev. 1997;61:141–149.
LeRoith D, Werner H, Beitner-Johnson D, Roberts CT. Molecular and cellular aspects of insulin-like growth factor I receptor. Endocrinol. Rev. 1995;16:143–163.
Levin SA, Grenfell B, Hastings A, Perelson AS. Mathematical and computational challenges in population biology and ecosystems science. Science 1997;275:334–343.
Li CC. A genetical model for emergenesis. Am. J. Hum. Genet. 1987;41:517–523.
Lieberman E, Torday J, Barbieri R, Cohen A, Van Vunakis H, Weiss ST. The association of in utero cigarette smoking to fetal lung maturation. Obstet. Gynecol. 1992;79:564–570.
Linask KK, D'Angelo M, Gehris AL, Greene RM. Transforming growth factor-β receptor profiles of human and murine embryonic palate mesenchymal cells. Exp. Cell Res. 1991;192:1–9.
Lyon MF, Kirby MC. Mouse chromosome atlas. In: Lyon MF, Raston S, Brown SDM, eds. Genetic Variants and Strains of the Laboratory Mouse. Oxford: Oxford University Press, 1996:881–924.
Matsushime H, Ewen ME, Strom DK, Kato JY, Hanks SK, Roussel ME, Sherr CJ. Identification and properties of an atypical catalytic subunit ($p34^{PSK\text{-}J3/cdk4}$) for mammalian D type G1 cyclins. Cell 1992;71:323–334.
Melnick M. Cleft lip (± cleft palate) etiology: A search for solutions. Am. J. Med. Genet. 1992;42:10–14.
Melnick M, Jaskoll T. H-2 haplotype and heterochronic orofacial morphogenesis in congenic mice: Consideration as a possible explanation for differential susceptibility to teratogenesis. J. Craniol. Genet. Dev. Biol. 1992;12:190–195.
Melnick M, Shields ED. Cleft lip and cleft palate. In: Melnick M, Shields ED, Burzynski NJ, eds. Clinical Dysmorphology of Oral-Facial Structures. Boston: John Wright-PSG, Inc., 1982:360–372.
Melnick M, Jaskoll T, Slavkin HC. Corticosteroid-induced cleft palate in mice and H-2 haplotype: Maternal and embryonic effects. Immunogenetics 1981a;13:443–450.
Melnick M, Jaskoll T, Slavkin HC. The association of H-2 haplotype with implantation, survival, and growth of murine embryos. Immunogenetics 1981b;13:303–308.
Melnick M, Jaskoll T, Marazita M. Localization of $H\text{-}2K^k$ in developing mouse palates using monoclonal antibody. J. Embryol. Exp. Morphol. 1982;70:45–60.
Melnick M, Chen H, Rich KA, Jaskoll T. Developmental expression of insulin-like growth factor II receptor in congenic mouse embryonic lungs: Correlation between IGF-IIR mRNA and protein levels and heterochronic lung development. Mol. Reprod. Dev. 1996;44:159–170.
Moats-Staats B, Price WA, Xu L, Jarvis HW, Stiles AD. Regulation of the insulin-like growth factor system during rat lung development. Am. J. Res. Cell. Mol. Biol. 1995;12:7035–7056.
Odekon LE, Blasi F, Rifkin DB. Requirement for receptor-bound urokinase in plasmin-dependent cellular conversion of latent TGF-β to TGF-β. J. Cell. Physiol. 1994;158:398–407.
Palsson BO. What lies beyond bioinformatics? Nature Biotechnol. 1997;15:3–4.
Pelton RW, Hogan BL, Millet DA, Moses HL. Differential expression of genes encoding TGFs β1, β2, and β3 during murine palate formation. Dev. Biol. 1990;141:456–460.
Penrose LS. The genetical background of common diseases. Acta Genet. 1953;4:257–265.
Pinsky L, DiGeorge AM. Cleft palate in the mouse: A teratogenic index of glucocorticoid potency. Science 1965;147:402–403.
Potchinsky M, Nugent P, Lafferty C, Greene RM. Effects of dexamethsone on the expression of transforming growth-factor-beta in mouse embryonic palatal mesenchymal cells. J. Cell. Physiol. 1996;166:380–386.
Rasco JF, Hood RD. Maternal restraint stress-enhanced teratogenicity of all-trans-retinoic acid in CD-1-mice. Teratology 1995;51:57–62.
Rosenzweig S, Blaustein FM. Cleft palate in A/J mice resulting from restraint and deprivation of food and water. Teratology 1970;3: 47–52.
Safra MJ, Oakley GP. Association between cleft lip with or without cleft palate and prenatal exposure to diazepam. Lancet 1975;2:478–480.
Salomon DS, Pratt RM. Involvement of glucocorticoids in the development of the secondary palate. Differentiation 1979;13:141–154.
Shields ED, Bixler D, Fogh-Andersen P. Cleft palate: A genetic and epidemiologic investigation. Clin. Genet. 1981;20:13–24.
Sklar MM, Keiss W, Thomas CL, Nissley SP. Developmental expression of the tissue insulin-like growth factor II/mannose 6-phosphate receptor in the rat. J. Biol. Chem. 1989;264:16733–16738.
Smokovits A. Differences in tissue plasminogen activator activity and plasmin inhibition between newborn and adult rat. Haemostasis 1980;9:52–64.
Smrzka OW, Faé I, Stöger R, Kurzbauer R, Fischer GF, Henn T, Weith A, Barlow DP. Conservation of a maternal-specific methylation signal at the human *IGF*2R locus. Hum. Mol. Genet. 1995;4:1945–1952.
Sokal RR, Rohlf FF. Biometry. San Francisco: W.H. Freeman, 1981.
Strohman RC. Epigenesis and complexity. The coming Kuhnian revolution in biology. Nature Biotechnol. 1997;15:194–200.
Szebenyi G, Rotwin P. The mouse insulin-like growth factor II/cation-independent mannose 6-phosphate (IGF-IIR/MPR) receptor gene: Molecular cloning and genomic organization. Genomics 1994;19:120–129.

Tanaka H, Asami O, Hayano T, Sasaki I, Yoshitake Y, Nishimura K. Identification of a family of insulin-like growth factor II secreted by cultured rat epithelial-like cell line 18,54-SF: Application of a monoclonal antibody. Endocrinology 1989;124:870–877.

Theiler K. The House Mouse. Atlas of Embryonic Development. New York: Springer-Verlag, 1989.

Vignon F, Rochefort H. Interactions of pro-cathepsin D and IGF-II on the mannose-6-phosphate/IGF-II receptor. Breast Cancer Res. Treat. 1992;22:47–57.

Vincek V, Sertie J, Zaleska-Rutezynska Z, Figuero F, Klein J. Characterization of H-2 congenic strains using DNA markers. Immunogenetics 1990;31:45–51.

Walker BE. Cleft palate produced in mice in human-equivalent dosage with triamcinolone. Science 1965;149:862–863.

Wang ZQ, Fund MR, Barlow DP, Wagner EF. Regulation of embryonic growth and lysosomal targeting by the imprinted *Igf*/*Mpr* gene. Nature 1994;372:464–467.

Xu Y, Goodyer CG, Deal C, Polychronakos C. Functional polymorphism in the parental imprinting of the human *IGF*2R gene. Biochem. Biophys. Res. Commun. 1993;197:747–754.

Zhan Y, Blanks JC, Hinton DR, Rich KA. Differing patterns of expression of insulin-like growth factor binding-proteins (IGFBPS) in the developing mouse retina. Invest. Ophthalmol. Visual Sci. 1994;35:1404a.